Front. Chem. Sci. Eng. 2016, 10(2): 265–272
DOI 10.1007/s11705-016-1570-6

RESEARCH ARTICLE

Plasma-enabled sensing of urea and related amides on polyaniline

Harinarayanan Puliyalil[1,2], Petr Slobodian[3], Michal Sedlacik[3], Ruhan Benlikaya[4], Pavel Riha[5], Kostya (Ken) Ostrikov[6,7,8], Uroš Cvelbar (✉)[1,2]

1 Jozef Stefan Institute (F4), Jamova cesta 39, 1000 Ljubjana, Slovenia
2 Jozef Stefan International Postgraduate School, Jamova cesta 39, 1000 Ljubjana, Slovenia
3 Centre of Polymer Systems, University Institute, Tomas Bata University, Trida T. Bati 5678, 76001 Zlin, Czech Republic
4 Department of Secondary Science and Mathematics Education, Faculty of Necatibey Education, Balikesir University, 10100 Balikesir, Turkey
5 Institute of Hydrodynamics, Academy of Sciences, Pod Patankou 5, 166 12 Prague 6, Czech Republic
6 Institute for Future Environments and Institute for Health and Biomedical Innovation, School of Chemistry, Physics and Mechanical Engineering, Queensland University of Technology, Brisbane, Queensland 4000, Australia
7 CSIRO-QUT Joint Sustainable Materials and Devices Laboratory, Commonwealth Scientific and Industrial Research Organization, New South Wales 2070, Australia
8 School of Physics, The University of Sydney, Sydney, New South Wales 2006, Australia

Abstract The atmospheric pressure plasma jet (APPJ) was used to enhance the sensitivity of industrially important polyaniline (PANI) for detection of organic vapors from amides. The gas sensing mechanism of PANI is operating on the basis of reversible protonation or deprotonation, whereas the driving force to improve the sensitivity after plasma modifications is unknown. Herein we manage to solve this problem and investigate the sensing mechanism of atmospheric plasma treated PANI for vapor detection of amides using urea as a model. The results from various analytical techniques indicate that the plausible mechanism responsible for the improved sensitivity after plasma treatment is operating through a cyclic transition state formed between the functional groups introduced by plasma treatment and urea. This transition state improved the sensitivity of PANI towards 15 ppm of urea by a factor of 2.4 times compared to the non-treated PANI. This plasma treated PANI is promising for the improvement of the sensitivity and selectivity towards other toxic and carcinogenic amide analytes for gas sensing applications such as improving material processing and controlling food quality.

Keywords gas sensing, urea, PANI, amides, plasma

Received December 31, 2015; accepted February 2, 2016

E-mail: uros.cvelbar@ijs.si

1 Introduction

For detection of toxic and carcinogenic gaseous analytes, the use of conducting polymers like polyaniline (PANI) is very important for promises of long-hold solutions and possibility toward commercial devices in industry. PANI is one of the best candidates for this purpose, because of its easy and low-cost synthesis, good environmental stability, and simple doping/dedoping process based on acid/base reactions [1,2]. The nature of PANI conductivity is explained by its ability to form polarons and cation radicals [3]. PANI sensors are largely reported for the sensing of volatile organic compounds which cause health issues such as allergy, irritation to eyes and skin, damage to kidneys and lungs, cancer and even death [4,6]. Our research focuses on polar molecules, especially the ones from amide group, which are mostly toxic and carcinogenic. The amides in the form of DMF (*N*,*N*-dimethylformamide), acrylamide, HMPA (hexamethylphosphoramide), urea (carbamide), etc. are found in materials or food and are hard to detect. Moreover, the sensitivity of the PANI against these analytes is not satisfactory.

To improve the sensing and solubility properties of PANI, various methods such as dopant utilization, chemical modification, and plasma treatment have been developed [7]. Up to date, only low pressure plasma treatment in glow discharge has been reported for the modification of the surface characteristics including chemical composition of PANI for improving its sensing

properties [8,9]. On the PANI surface, various extend can be achieved predominantly by carbon oxidation after PANI is exposed to various low pressure plasmas. Oxygen plasma treated PANI surface showed 30% increase in the signal response to H_2 (10 ppm), whereas the same treatment decreased the sensitivity towards NH_3 [10]. This clearly indicated that the sensor operates through different mechanisms towards various analytes. There were many other reports on enhanced sensing properties of PANI or its composites towards various volatile organic molecules by plasma treatment [10−12]. However, the exact sensing mechanism of plasma treated PANI is still unclear and the improvements are unsatisfactory.

Among various amide analytes, urea is practically nontoxic and a good model molecule for testing amide detection. The detection of urea molecules is typically achieved by different techniques including potentiometry, amperometry, colorometry or impedometry [13]. Urea is also determined by using high performance liquid chromatography (anion-exchange column and neutral phosphate buffer) to map its thermal decomposition products [14]. Similarly the analysis of urea by a polypyrrole based detector was reported by sensing NH_3 gas generated as a by-product of urea decomposition [15]. However, none of these methods allows direct sensing of urea vapour, and consequently amides arising vapours. To the best of our knowledge, the direct detection of urea vapour has not been reported yet. Herein, we propose a new approach based on an atmospheric pressure plasma instead of low pressure plasmas which other researchers failed on, and targeted very specific functionalization of PANI to increase its sensitivity for urea vapours and other amides. We have improved sensing mechanism of plasma modified PANI through a cyclic transition state between the functional groups generated after plasma treatment and the atoms of the guest amide molecules.

2 Experimental

2.1 Materials and PANI preparation

PANI was prepared via oxidative polymerization from ammonium persulfate (APS, purity = 98%, purchased from Sigma-Aldrich Inc., USA) and aniline hydrochloride (purity ⩾ 99%, purchased from Fluka, Switzerland), which were used without further purification. Acetone (p.a.) used for degreasing and cleaning the commercial polyethylene terephthalate (PET) foil (thickness 0.1 mm) was purchased from Penta Ltd., Czech Republic.

Standard PANI emeraldine was prepared according to the procedure described in the previous paper [16]. The PET foil was formerly washed by dipping it in acetone for 30 min and dried. In course of polymerization 0.2 mol/L aniline hydrochloride was mixed with 0.25 mol/L APS in water and briefly stirred. The treated PET foil was inserted into batch with polymerized reagents and the reaction was conducted for 24 h at room temperature. The PET foil acts as a substrate for the PANI emeraldine salts which forms as a thin layer firmly adhered onto PET surface. The PET support coated with PANI film was afterwards rinsed with acetone and dried in the vacuum at 60 °C for 24 h.

The samples were treated with an atmospheric pressure plasma jet (APPJ) created with electrode discharge within pure He 5.0 as the plasma gas. The plasma electrode was made of Cu wire with a diameter of 0.1 mm, which was connected to the power supply operating at 25 kHz, and more details could be find elsewhere [17,18]. The PANI layer was treated for 1.5 min under the plasma jet at the distance of 20 mm from jet nozzle to substrate, which was generated at a He gas flow rate of 35 sccm. After the treatment process, the resistivity of the PANI layer was increased from 70 to 1200 kΩ.

2.2 Characterization methods

The chemical composition of PANI was examined with Fourier transform spectroscopy (FTIR, Thermo Scientific, USA). The FTIR spectra were recorded using attenuated total reflectance (ATR) technique with germanium crystal in the range 600−4000 cm^{-1} at 64 scans per spectrum at 2 cm^{-1} resolution. The X-ray photoelectron spectroscopy (XPS) analyses were carried out on the PHI-TFA XPS spectrometer produced by Physical Electronics Inc. at a depth about 3−5 nm from the top surface. Both XPS and FTIR measurements on the urea exposed samples were carried out immediately after taking them out from the testing gas chamber.

2.3 Electrical resistance measurements

The electrical resistance of stripes cut out from PANI/PET was measured along the specimen length by the two-point technique using multimeter Sefram 7338. The stripe was placed on a planar holder with Cu electrodes fixed on both sides of the specimen (length 20 mm, distance 10 mm between electrodes, and width of strips 10 mm). Time-dependent electrical resistance measurements were performed during adsorption and desorption cycles. In the former case the holder with the specimen was quickly transferred into an airtight flask with urea vapors sublimated from layer of its solid crystals (~3 g) at the bottom [19,20]. The measurements were conducted in 15 ppm of urea vapors at atmospheric pressure and 25 °C. After 6 min, the holder was promptly removed from the flask, and for the next 6 min the sample was measured in the mode of desorption. This was repeated six times in consecutive cycles and for 10 samples. Then it was repeated again for plasma treated specimens. The measurements was also performed for longer times (20 min) of adsorption/desorption cycle to observe full surface loading or relaxation.

3 Results and discussion

The adsorption of urea molecules onto PANI surface increased the electrical resistance due to the deprotonation from the conducting form of PANI. For urea, the deprotonation may occur through two possible coordinating sites with the electron deficient center of PANI: either the nitrogen atom or oxygen atom. The electron density of urea is located more on the oxygen because of the π electron conjugation between the lone pairs of nitrogen and the oxygen within the molecular chain [21]. These typical responses are time-dependent and can be presented as sensitivity or gas response, S, defined as following equation,

$$S = \frac{R_g - R_a}{R_a} = \frac{\Delta R}{R_a}$$

where R_a represents specimen resistance in air, R_g resistance of the specimen exposed to gas/vapor, and ΔR the resistance change.

The observed sensitivity response time for the non-treated samples was 9 s (±1 s), whereas it was reduced to 6 s (±0.7 s) for the samples after plasma surface modification. The sensitivity response time was measured as the time required for the sensor to show the change in resistivity as observed from the sensitivity curve. Moreover, the observed signal response was 2.4 times higher for the plasma modified samples than for the non-treated samples. The response time for 6 consecutive cycles for both plasma treated and non-treated samples is presented in Fig. 1.

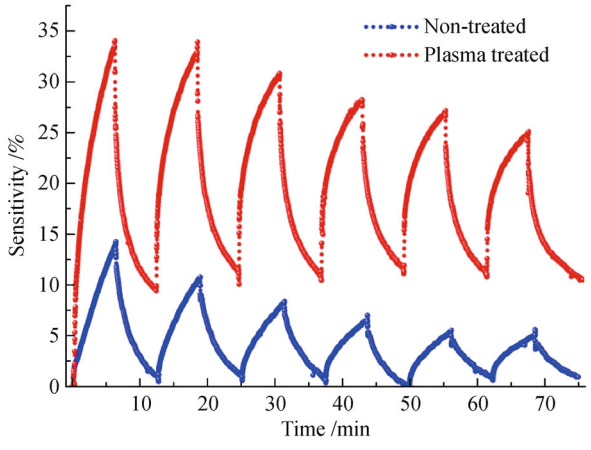

Fig. 1 Signal response curve for non-treated and plasma treated PANI for urea vapor

To disclose the sensing mechanism and reveal how plasma modifications improve sensitivity, the detailed investigation on the chemical structures was essential. XPS is one of the best tools to detect the chemical changes on the surface within a depth of ~5 nm. The XPS results indicated a significant increase in the oxygen content on the surface of the PANI layer after the plasma treatments. C1s deconvolution of non-treated and plasma treated samples before and after exposing to urea is presented in Fig. 2. After plasma treatment, the peaks corresponding to oxidized carbon bonds (carboxylic group) appeared below 290 eV in the C 1s peak with a significant intensity, whereas the intensities corresponding to C–C or C–H bond types at < 285 eV decreased [10,22]. No significant changes were observed in the C 1s spectrum of the non-treated sample before and after exposing to urea vapor. On the other hand, for the plasma treated sample, the intensity of C 1s peak slightly increased after exposing to urea vapor due to the aging effect of functional groups after plasma treatment [23]. The oxidation of the carbon on the aromatic rings reduced the conductivity of the PANI layer because of a decrease in the electron conjugation. The sensible argument is that the electronegative oxygen attached to the aromatic ring removed the electron density towards itself and made the π electrons less available for ring conjugation.

The deconvolution of N 1s peak for the non-treated sample revealed that the chemical state of nitrogen was dominated by four types of bonding states (Fig. 3(A)). The major peaks at 398.7 and 399.6 eV corresponds to imine (=N–) and benzenoid amine (–NH–), respectively [24]. The peaks at > 400 eV are assigned to protonated nitrogen — a positively charged N atom of the conjugated ring. However, the relative intensity of the peak at ~ 401.3 eV significantly increased after the plasma exposure. This increase is partially in contradiction with the reduced polymer conductivity after plasma treatment, and thus is not because of the increased protonated nitrogen atoms on the chain. The peak above 401 eV is characteristic of nitrogen bonded to highly electronegative atoms such as oxygen [25]. Therefore, the intensity increase of the peak at above 401 eV is probably due to the oxidation of nitrogen in the polymer chain which is in accordance with the binding energies of (C_6H_5)–N=O states as reported by Batich and Donald [26]. In addition to this, the origin of these states could be also connected to various oxidized NO_x species generated during the atmospheric pressure discharge, which are chemisorbed on the surface [17,18]. So, the peak at > 401 eV could be linked to the various contributions from multiple species on the surface linked to protonated amine or delocalized nitrogen in protonated imine. After the plasma treatment, the intensity of =N– bond significantly decreased compared to –NH– bond, where this change in intrinsic oxidation state was accompanied by the hydrolysis of the polymer chain under the influence of the reactive oxidants in atmospheric pressure plasma [27]. In contrary to the non-treated sample, plasma treated sample showed a reversal of the chemical state after exposing to urea vapor. There is no possible chemical bonding between the guest and host molecules at room temperature, which holds up the aging effect of the sample surface.

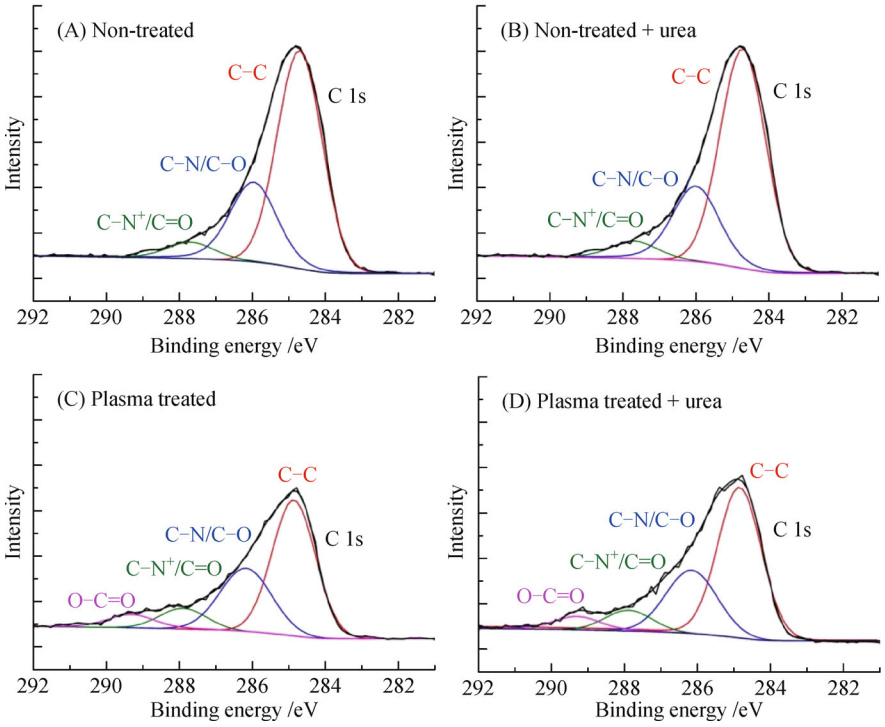

Fig. 2 Deconvoluted C 1s spectra for non-treated PANI (A) before and (B) after exposing to urea, and plasma treated PANI (C) before and (D) after exposing to urea

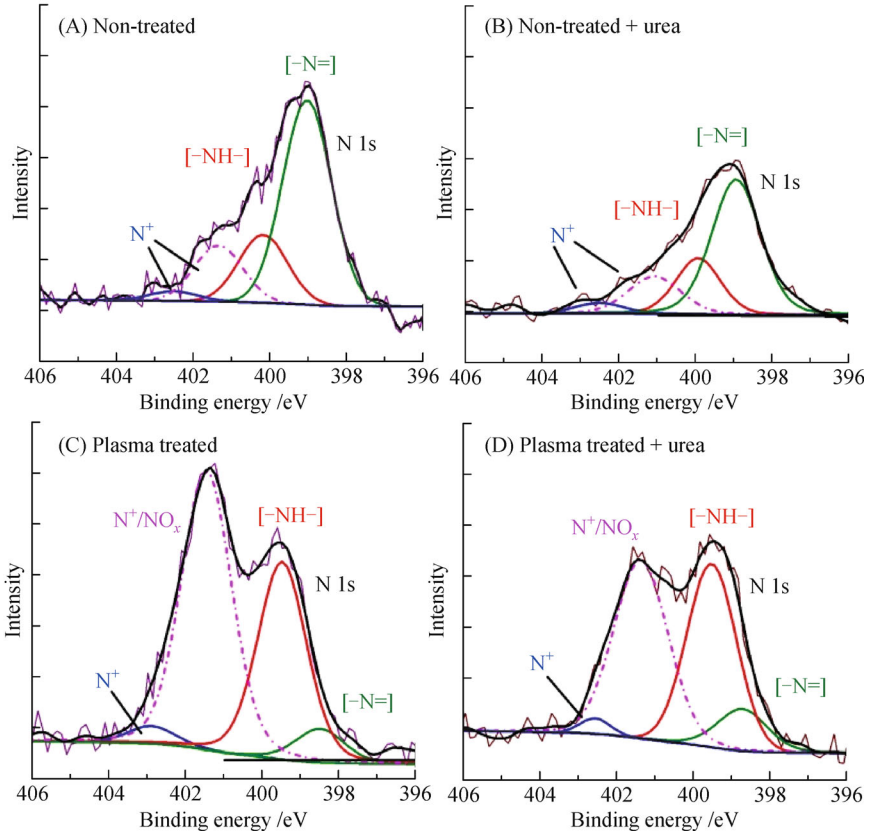

Fig. 3 Deconvoluted N 1s spectra for non-treated PANI (A) before and (B) after exposing to urea, and plasma treated PANI (C) before and (D) after exposing to urea

The evaluation by XPS alone was not sufficient to study the exact interactions between the guest and the host. Because the measurements were performed at ultra-high vacuum, the guest molecule could be desorbed from the surface before the signals were collected. In addition, XPS is not the best technique to understand the surface chemistry in detail. For better understanding of the sensing mechanisms, more precise and faster technique FTIR was used. FTIR spectra show two peaks at 1582 and 1498 cm^{-1} belonging to quinonoid and benzenoid ring deformations, respectively (Fig. 4). The band observed at 1234 cm^{-1} is assigned to C–N group in the benzenoid ring when the one at 1309 cm^{-1} belongs to C=N vibration mode of the quinonoid ring. The bands at around 1152 and 817 cm^{-1} correspond to C–H in-plane and out-of-plane deformations on the aromatic rings, respectively. The small peaks observed at 1086 and 706 cm^{-1} could belong to C–H vibration and out-of-plane ring bending in mono substituted aromatic rings respectively [28]. When comparing the spectra of non-treated PANI and plasma treated PANI, two major differences were observed: i) The transformation of the peak at 1086 cm^{-1} in the spectrum of PANI to the shoulder in that of plasma treated PANI, and ii) the split-up of the small peak at around 706 cm^{-1} in the spectrum of PANI to two peaks in that of plasma treated PANI. The peak at 1153 cm^{-1} exhibited a shift towards lower wavenumber after the plasma treatment. When the analysis was done for the non-treated and plasma treated samples, immediately after exposing to urea vapor, the spectra disclosed that the interactions of pure PANI and plasma treated PANI with urea are different from each other. Pure PANI interacts with urea through the C–N in the benzenoid, whereas in the interaction of plasma treated PANI with urea, the aromatic ring current also changes slightly.

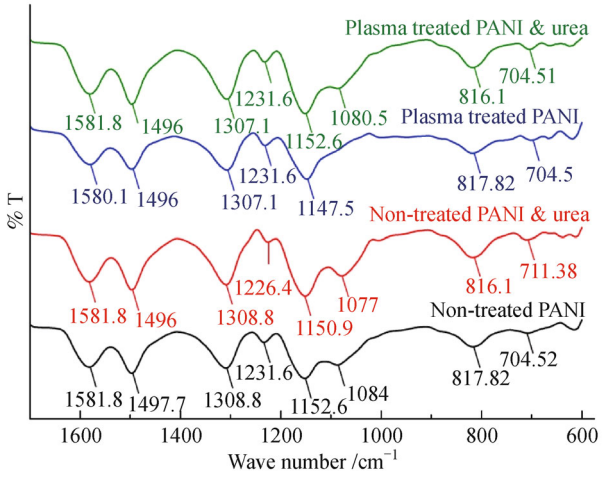

Fig. 4 FTIR spectra for non-treated and plasma treated PANI samples before and after detection of urea molecules

The results from both XPS and FTIR measurements revealed that the plasma treatment introduced oxygen functionalities on to the aromatic ring and the interaction of the plasma treated samples disturbed the π electron cloud from the aromatic ring. In the case of pure PANI, the sensing only affected the C–N bonds in the benzoid ring, where the sensing mechanism was only operated by the removal of the proton from the nitrogen atom. These observations summed up to a conclusion that the plasma functionalization has some influence on the sensing mechanism. The plausible reason for the increased sensitivity of plasma treated samples should be through some intermediate transition state which facilitated the adsorption of PANI onto the surface and stabilized the guest-host transition state. The electron rich oxygen atom of the urea molecule will interact with the electron deficient nitrogen atom (or proton) of the polymer chain. At the same time, the nitrogen atom of urea, which possess a slight positive charge by contributing the electron density for the electron conjugation with the carbonyl carbon, would coordinate with the plasma functionalized oxygen atom attached to the aromatic ring of the polymer. This would give rise to a cyclic seven membered transition state. The plausible structures for the non-treated and plasma treated samples and their corresponding intermediate states on interaction with urea molecule are schematically presented in Figs. 5(A–D). On the other hand, the possibility a six membered coordination state by the interaction of oxygen from the PANI with the amide carbon is also possible. When such an intermediate state is formed, the electron density from the functionalized oxygen would be shifted towards the urea molecule. To compensate this charge, oxygen would exert more electrostatic attraction to remove the electron density from the π electron cloud of the aromatic ring. Such cyclic intermediate states are widely used to explain the mechanism in various reactions [29]. Representative examples can be found in transition metal complex mediated C–H bond activation reactions where the cyclic ring states provide additional energy stabilization to the intermediate species [30–32]. During the transition state formation, the electron density from the unsaturated bonds shifts towards the electron withdrawing center, which is in agreement with the FTIR results. The stability and existence of such transition states were both experimentally and theoretically proved. In the present example of PANI, it has the predominant possibility to form such transition states.

A short overshooting of the signals immediately after exposing to the analyte vapor is attributed to the rapid increase in the concentration of the analyte in the interacting zone [10]. Nevertheless, this effect is more noticeable for the plasma treated sample. The cyclic transition state increases the guest-host interactions and thereby holds the urea closer into the proximity of the PANI. Such an effect is completely absent for the pure PANI.

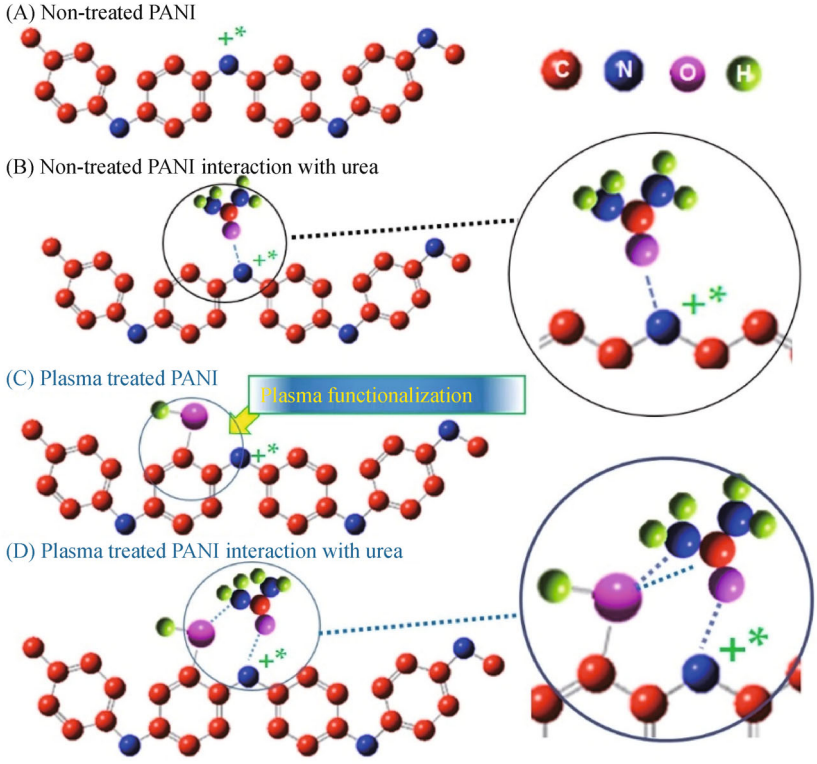

Fig. 5 Schematic view of the sensing mechanism: (A) Non-treated PANI, (B) interaction of the non-treated PANI with urea molecule, (C) plasma functionalized PANI, and (D) plasma functionalized PANI forming ring structure with the urea molecule

After revealing this vapor gas sensing mechanism, it is possible to extend this work further to other more toxic and harmful amide molecules. Because cyclic transition states are formed from the interaction of –N– atoms and O functional groups on C rings of PANI with –N–C = O of guest amide molecules, this mechanism could be proposed and used for other amides like DMF, HMPA and acrylamide. These cyclic transition states proposed are listed in the Fig. 6. Even though six membered transition states are energetically easier to form than a seven membered ring, one can propose an ease formation of both six and seven membered transition states while considering urea or acrylamide. However, in the case of the other amides including HMPA or DMF, the substituents on the nitrogen atoms are bulky methyl groups. This can restrict the formation of nitrogen atom involvement in the

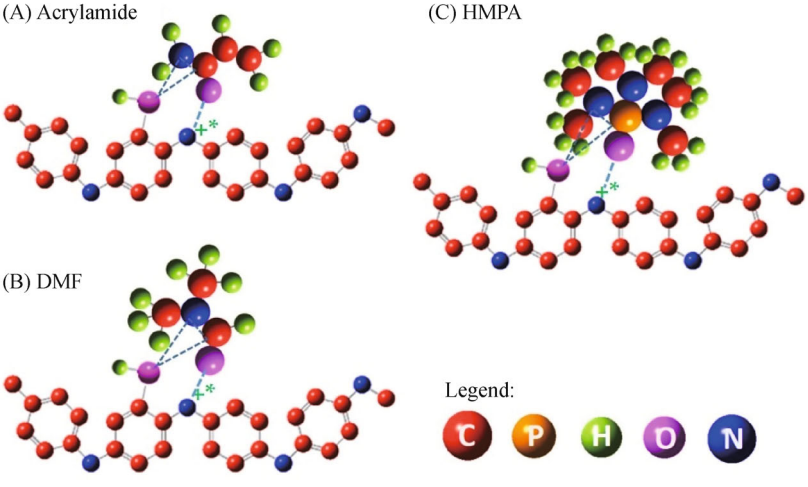

Fig. 6 Transition cyclic states formed from PANI and other amide molecules: (A) Acrylamide, (B) DMF, and (C) HMPA

transition state due to steric hindrance. Thus in the case of DMF, the coordination is possible through the carbonyl carbon. Likewise in the case of HMPA, the favored six membered transition state will be proceeding strictly via coordination though the electropositive, steric free phosphorous atom. When these cyclic transition states are formed the sensitivity of PANI against detection amide molecules will be increased, since the guest-host interactions will hold the molecules more in the proximity of polymer and enable their better detection.

4 Conclusions

The gas vapor detection of amides with urea as a model is presented, where the surface of PANI is designed to boost sensitivity. This conceptually novel approach utilizes the very simple He atmospheric pressure plasma jet and targeted functionalization of PANI, and thus enables higher sensitivity due to formation of cyclic transition states between the functional groups generated after plasma treatment with the atoms of the guest molecules. The existence of cyclic transition states was confirmed through the surface analyses using both XPS and FTIR. Moreover, because the cyclic transition states are formed from the interaction of –O functional groups and –N– atoms of plasma treated PANI with N–C = O of guest molecule, a wider application is promising for most of amides such as DMF, HMPA and acrylamide. However, simulations on the stability of various transition states are needed for more precise optimization of the sensing mechanism for future applications such as commercial devices enabling to detect potential environment risks, or to better control food quality against harmful substances.

Acknowledgements This project was supported by the Slovenian Research Agency (ARRS) project L2-6769, and by the Ministry of Education, Youth and Sports of the Czech Republic—program NPU I (LO1504). H.P thanks Jozef Stefan International Postgraduate School (MPŠ) for the PhD grant. KO thanks the Australian Research Council and CSIRO Science Leadership Program for partial support.

References

1. Macdiarmid A G, Chiang J C, Richter A F, Epstein A J. Polyaniline: A new concept in conducting polymers. Synthetic Metals, 1987, 18: 285–290
2. Hao B, Li L, Wang Y, Qian H, Tong G, Chen H, Chen K. Electrical and microwave absorbing properties of polypyrrole synthesized by optimum strategy. Journal of Applied Polymer Science, 2013, 127: 4273–4279
3. Trivedi D C. Polyanilines. In: Nalwa H S, ed. Handbook of Organic Conductive Molecules and Polymers, vol. 2. New Jersey: John Wiley & Sons, 1997, 505
4. Ayad M M, El-Hefnawey G, Torad N L. A sensor of alcohol vapours based on thin polyaniline base film and quartz crystal microbalance. Journal of Hazardous Materials, 2009, 168: 85–88
5. Nicolas-Debarnot D, Poncin-Epaillard F. Polyaniline as a new sensitive layer for gas sensors. Analytica Chimica Acta, 2003, 475: 1–15
6. Zhang X, Qin Z, Liu X, Liang B, Liu N, Zhou Z, Zhu M. Flexible sensing fibers based on polyaniline-coated polyurethane for chloroform vapor detection. Journal of Materials Chemistry. A, Materials for Energy and Sustainability, 2013, 1: 10327–10333
7. Jaymand M. Recent progress in chemical modification of polyaniline. Progress in Polymer Science, 2013, 38: 1287–1306
8. Kang E T, Ma Z H, Tan K L, Zhu B R, Uyama Y, Ikada Y. Surface modification and functionalization of electroactive polymer films. Polymers for Advanced Technologies, 1999, 10: 421–428
9. Kang E T, Kato K, Uyama Y, Ikada Y. Plasma treatment of polyaniline films: Effect on the intrinsic oxidation states. Journal of Materials Research, 1996, 11: 1570–1573
10. Kunzo P, Lobotka P, Micusik M, Kovacova E. Palladium-free hydrogen sensor based on oxygen-plasma-treated polyaniline thin film. Sensors and Actuators. B, Chemical, 2012, 171-172: 838–845
11. Yoo K P, Kwon K H, Min N K, Lee M J, Lee C J. Effects of O_2 plasma treatment on NH_3 sensing characteristics of multiwall carbon nanotube/polyaniline composite films. Sensors and Actuators. B, Chemical, 2009, 143: 333–340
12. Du H Y, Wang J, Yao P J, Hao Y W, Li X G. Preparation of modified MWCNTs-doped PANI nanorods by oxygen plasma and their ammonia-sensing properties. Journal of Materials Science, 2013, 48: 3597–3604
13. Koebel M, Elsener M. Determination of urea and its thermal decomposition products by high-performance liquid chromatography. Journal of Chromatography. A, 1995, 689: 164–169
14. Bertocci P, Compagnone D, Palleschi G. Amperometric ammonium ion and urea determination with enzyme-based probes. Biosensors and Bioelectronics, 1996, 11: 1–10
15. Palmqvist E, Kriz C B, Svanberg K, Khayyami M, Kriz D. DC-resistometric urea sensitive device utilizing a conducting polymer film for the gas-phase detection of ammonia. Biosensors & Bioelectronics, 1995, 10: 283–287
16. Stejskal J, Gilbert R G. Polyaniline: Preparation of a conducting polymer (IUPAC technical report). Pure and Applied Chemistry, 2002, 74: 857–867
17. Zaplotnik R, Bišćan M, Kregar Z, Vesel A, Cvelbar U, Mozetic M, Milošević S. Influence of a samples surface on single electrode atmospheric pressure plasma jet parameters. Spectrochemica acta B, 2014, 103/104: 124–130
18. Zaplotnik R, Kregar Z, Bišćan M, Vesel A, Cvelbar U, Mozetic M, Milošević S. Multiple vs. single harmonics AC-driven atmospheric pressure plasma jet. Europhysics Letters, 2014, 106: 25001
19. Niu L, Luo Y, Li Z. A highly selective chemical gas sensor based on functionalization of multi-walled carbon nanotubes with poly (ethylene glycol). Sensors and Actuators. B, Chemical, 2007, 126: 361–367
20. Slobodian P, Riha P, Lengalova A, Svoboda P, Saha P. Multi-wall carbon nanotube networks as potential resistive gas sensors for organic vapor detection. Carbon, 2011, 49: 2499–2507
21. Wen N, Brooker M H. Urea protonation: Raman and theoretical study. Journal of Physical Chemistry, 1993, 97: 8608–8616
22. Kang E T, Ma Z H, Tan K L, Zhu B R, Uyama Y, Ikada Y. Surface

modification and functionalization of electroactive polymer films. Polymers for Advanced Technologies, 1999, 10: 421–428

23. Puliyalil H, Cvelbar U, Filipič G, Petrič A D, Zaplotnik R, Recek N, Mozetič M, Thomas S. Plasma as a tool for enhancing insulation properties of polymer composites. RSC Advances, 2015, 5: 37853–37858
24. Qaiser A A, Hyland M M, Patterson D A. Surface and charge transport characterization of polyaniline-cellulose acetate composite membranes. Journal of Physical Chemistry B, 2011, 115: 1652–1661
25. Peng H, Mo Z, Liao S, Liang H, Yang L, Luo F, Song H, Zhong Y, Zhang B. High performance Fe- and N- doped carbon catalyst with graphene structure for oxygen reduction. Scientific Reports, 2013, 3: 1765
26. Batich C D, Donald D S. X-ray photoelectron spectroscopy of nitroso compounds: Relative ionicity of the closed and open forms. Journal of the American Chemical Society, 1984, 106: 2758–2761
27. Angelopoulos M, Asturias G E, Ermer S P, Ray A, Scherr E M, Macdiarmid A G, Akhtar M, Kiss Z, Epstein A J. Polyaniline: Solutions, films and oxidation state. Molecular Crystals and Liquid Crystals Incorporating Nonlinear Optics, 1988, 160: 151–163
28. Trchová M, Stejskal J. Polyaniline: The infrared spectroscopy of conducting polymer nanotubes. Pure and Applied Chemistry, 2011, 83: 1803–1817
29. Boer F P, Shannon T W, Mclafferty F W. Electronic structure of the six-membered cyclic transition state in some gamma hydrogen rearrangements. Journal of the American Chemical Society, 1968, 90: 7239–7248
30. Ostrikov K, Yoon N J, Rider A E, Vladimirov S V. Two-dimensional simulation of nanoassembly precursor species in $Ar + H_2 + C_2H_2$ reactive plasmas. Plasma Processes and Polymers, 2007, 4: 27–40
31. Arockiam P B, Bruneau C, Dixneuf P H. Ruthenium (II)-catalyzed C–H bond activation and functionalization. Chemical Reviews, 2012, 112: 5879–5918
32. Dang Y, Qu S, Nelson J W, Pham H D, Wang Z X, Wang X. The mechanism of a ligand-promoted sp^3 C–H activation and arylation reaction via palladium catalysis: Theoretical demonstration of a Pd (II)/Pd(IV) redox manifold. Journal of the American Chemical Society, 2015, 137: 2006–2014